Protein NMR

International Edition: DOI: 10.1002/anie.201706060
German Edition: DOI: 10.1002/ange.201706060

Bacteriophage Tail-Tube Assembly Studied by Proton-Detected 4D Solid-State NMR

*Maximilian Zinke, Pascal Fricke, Camille Samson, Songhwan Hwang, Joseph S. Wall, Sascha Lange, Sophie Zinn-Justin, and Adam Lange**

Abstract: *Obtaining unambiguous resonance assignments remains a major bottleneck in solid-state NMR studies of protein structure and dynamics. Particularly for supramolecular assemblies with large subunits (>150 residues), the analysis of crowded spectral data presents a challenge, even if three-dimensional (3D) spectra are used. Here, we present a proton-detected 4D solid-state NMR assignment procedure that is tailored for large assemblies. The key to recording 4D spectra with three indirect carbon or nitrogen dimensions with their inherently large chemical shift dispersion lies in the use of sparse non-uniform sampling (as low as 2 %). As a proof of principle, we acquired 4D (H)COCANH, (H)CACONH, and (H)CBCANH spectra of the 20 kDa bacteriophage tail-tube protein gp17.1 in a total time of two and a half weeks. These spectra were sufficient to obtain complete resonance assignments in a straightforward manner without use of previous solution NMR data.*

Solid-state NMR is a spectroscopic technique that can be applied to investigate the structure and dynamics of insoluble proteins, including amyloid fibrils,[1,2] functional supramolecular assemblies,[3,4] and membrane-integrated proteins,[5] at atomic resolution.[6–8] In contrast to other methods, solid-state NMR does not require long-range order and can operate with proteins under in vivo conditions, for instance membrane proteins can be studied in lipid bilayers[9,10] or in nanodiscs.[11] In contrast to solution NMR, solid-state NMR is not limited by the size of the protein since solid-state NMR linewidths under magic-angle spinning (MAS) conditions do not depend on molecular tumbling in solution, which decreases with increasing protein size. However, due to the inherently large linewidths in solid-state NMR and the resulting spectral crowding, studies of fully-labeled large proteins (>150 residues) have remained a challenge to date.

Phages are viruses that infect bacteria. Since their discovery, they have attracted interest as tools for combating pathogenic bacteria in clinical treatments. Increasing antibiotic resistance and a lack of new antibiotics in the pipeline makes it imperative to search for alternatives.[12] Phage therapy exploits the high specificity of phages towards their bacterial hosts while remaining harmless to the symbiotic gut flora. It is currently being used in Russia, Georgia, and Poland, for example, for treating methicillin-resistant *Staphylococcus aureus* (MRSA).[13] To further develop this therapy, the mechanisms of attachment to the host cell, infection, and replication need to be understood on an atomic level.

gp17.1 is the major tail protein of the bacteriophage SPP1. Polymerized gp17.1 monomers form a hollow tube that connects the capsid with the phage tail tip (Figure 1 B). The phage tail is required for DNA release into the host cell.[14,15]

A preliminary analysis of gp17.1 by solid-state NMR showed that the β-sheet content increases upon polymeri-

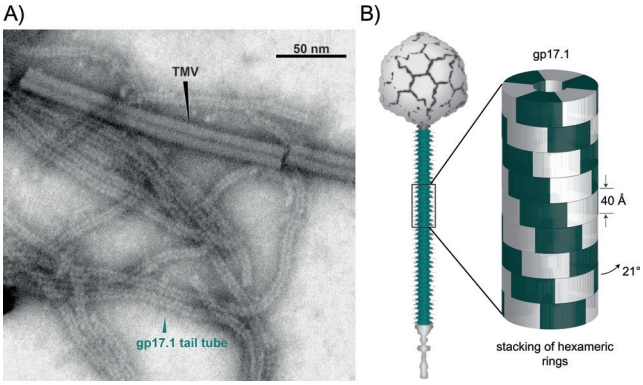

Figure 1. The tail-tube protein gp17.1 of bacteriophage SPP1. A) A negative-stain electron micrograph of purified gp17.1 after three weeks of polymerization, with tobacco mosaic virus (TMV) reference particles for comparison. The tail-tube periodicity was measured to be around 40 Å using the program PCMass. B) Schematic organization of the bacteriophage SPP1. The tail tube (turquoise), consisting of polymerized gp17.1 monomers, connects the icosahedral capsid containing the double-stranded DNA to the remote tip complex at the distal end of the tail. The expanded region illustrates the structural organization of the hollow tube. Hexameric rings are stacked on top of each other and rotated relative to each other by 21°.[15]

[*] M. Zinke, P. Fricke, S. Hwang, Dr. S. Lange, Prof. Dr. A. Lange
Department of Molecular Biophysics
Leibniz-Forschungsinstitut für Molekulare Pharmakologie (FMP)
Berlin (Germany)
E-mail: alange@fmp-berlin.de
Prof. Dr. A. Lange
Institut für Biologie, Humboldt-Universität zu Berlin
Berlin (Germany)
C. Samson, Dr. S. Zinn-Justin
Institute for Integrative Biology of the Cell (I2BC), CEA, CNRS
Université Paris-Sud, Université Paris-Saclay
Gif-sur-Yvette Cedex (France)
Dr. J. S. Wall
Brookhaven National Laboratory, Upton, NY (USA)
Supporting information and the ORCID identification number(s) for the author(s) of this article can be found under: https://doi.org/10.1002/anie.201706060.

zation of the monomeric subunit.[15] Due to the large size of gp17.1 (177 residues) and the previous restriction of solid-state NMR to ^{13}C-detected methods, a full chemical-shift assignment could not be obtained. Therefore, we set out to study gp17.1 by high-dimensional ^{1}H-detected solid-state NMR.

MAS at more than or equal to 40 kHz and dilution of the proton network by deuteration of proteins (protons present only at all labile sites/100 % back-exchanged) allows the collection of well-resolved ^{1}H-detected solid-state NMR spectra. ^{1}H-detection expands the classic ^{13}C-detected experiments with an extra dimension and conveys eight-fold enhanced sensitivity due to the four-fold higher gyromagnetic ratio of protons. However, the enhancement also depends on other parameters, such as the active volume of the rotor, MAS rates, and decoupling efficiencies. Recently, we proposed a protocol consisting of a set of five 3D ^{1}H-detected correlation experiments to fully assign protein backbone resonances. The protocol is based on earlier work by several groups[16–19] and consists of 3D (H)CANH, (H)COCA(N)H, and (H)CBCA(N)H experiments to correlate intraresidual HN, N, Cα, CO, and Cβ resonances (residue *i*), and 3D (H)CONH and (H)CACO(N)H experiments to correlate those resonances with the Cα and CO resonances of the previous residue (*i*-1).[20]

Prior to this, four-dimensional (4D) "out-and-back" type (H)CACONH and (H)COCANH experiments had been developed by our group and successfully applied to 20 % proton back-exchanged type III secretion needles.[21] In an adapted version more suitable for deuterated, 100 % back-exchanged, or fully protonated samples (i.e. non "out-and-back"), these 4D experiments were recently applied in the successful analysis of fully protonated Tau-paired helical filaments.[22,23] Due to the high number of points in the indirect dimensions, 4D experiments are recorded in a non-uniformly sampled fashion by omitting points in the indirect dimensions.[24] Using this method increases sensitivity, which facilitates working with signals of a wide dynamic range and/or weak through-space cross-peaks.[25,26] Missing spectral points have to be reconstructed by methods such as maximum entropy,[27] multi-dimensional decomposition,[28] or compressed sensing.[29] However, reconstruction methods are known to introduce spectral artifacts that appear as non-genuine peaks. These can interfere with the detection of low-intensity genuine peaks.[30] We note that in assignment experiments with magnetization transfer in a defined direction (e.g. (H)→CA→CO→N→H), only one strong peak of interest for each residue is expected, which helps to differentiate between real peaks and artifacts. This situation is easier to resolve than in the case of 4D spectra designed for the detection of distance restraints, for instance between NH pairs, where a large number of cross peaks for each NH pair may be expected.[31,32] Nevertheless, it is particularly important to be able to reliably distinguish artifact peaks appearing in reconstructed 4D spectra from real peaks.

Here, we complement the 4D (H)CACONH and (H)COCANH spectra by the addition of a 4D (H)CBCANH spectrum. Additionally, in our new assignment approach, two uniformly sampled 3D spectra are recorded. The particular combination of these five experiments allows easy handling of the data during analysis: The 3D spectra are used to navigate in the 4D space and to separate genuine peaks from artifacts in the reconstructed 4D spectra by limiting the number of unknown dimensions to one (See Figure S1 in the Supporting Information, which shows an exceptional example of a low signal-to-noise genuine peak among artifacts). As a proof-of-principle, we report the full assignment of all observed peaks of the 20 kDa major phage tail protein gp17.1 using a total NMR experimental time of only two and a half weeks.

For this purpose, the major tail protein gp17.1 was recombinantly overexpressed in *E. coli* in a fully deuterated medium containing ^{13}C,D$_7$-glucose and ^{15}ND$_4$Cl as the sole carbon and nitrogen sources (see detailed experimental methods in the Supporting Information). After 3 weeks of polymerization, the tail tubes were pelleted by ultracentrifugation and transferred into a 1.9 mm solid-state NMR rotor for analysis. Negative-stain electron microscopy (EM) analysis of the sample reveals an organization consistent with previous experiments:[14] Rings with a thickness of around 40 Å are stacked on top of each other to form the hollow tail tube (Figure 1 A). Our recombinant tubes are thus indistinguishable by EM from native tubes in the context of fully assembled phages.[15]

Solid-state NMR experiments were conducted at 40 kHz MAS in a 1.9 mm rotor at an external magnetic field strength of 900 MHz. Figure 2 shows the "fingerprint" 2D (H)NH spectrum with indicated linewidths for an isolated resonance.

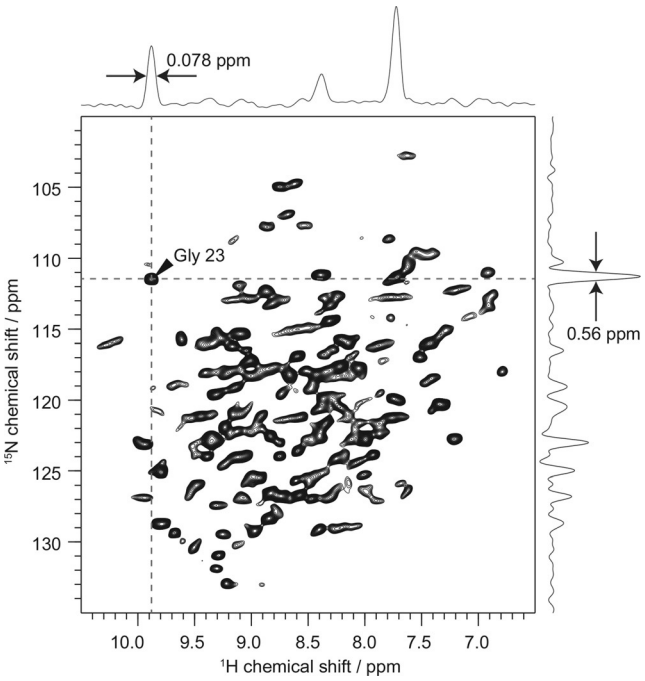

Figure 2. 2D (H)NH solid-state NMR correlation spectrum of gp17.1 tubes at 40 kHz MAS and 900 MHz external magnetic field strength. The linewidths of the assigned Gly23 residue correspond to data processed with a squared sine window function with a shift of 45°. Linewidths obtained without window functions are similar: 0.079 ppm for ^{1}H and 0.49 ppm for ^{15}N.

Although the spectral quality is good, spectral crowding occurs due to the high number of residues (177 without the His-tag, which cannot be observed in the cross-polarization-based experiment). Attempts to assign this protein with the strategy described in Fricke et al.[20] using a set of five 3D experiments were unsuccessful, since a large number of peaks (≈40%) could not be unambiguously assigned using this method. Therefore, this approach was abandoned in favor of the method described in this paper.

This new assignment strategy is based on the acquisition of two 3D and three 4D correlation spectra. Figure 3 illustrates the benefit of 4D NMR experiments: The spectral crowding in 2D (H)CB(CAN)H and even in 3D (H)CB(CA)NH spectra makes analysis very cumbersome and sometimes impossible. In contrast, the 4D (H)CBCANH spectrum allows fast and unambiguous assignment and can be recorded in nearly the same time as the 3D version provided that a non-uniform sampling approach is followed.

As shown in Figure 4, the 3D (H)CANH and (H)CONH spectra are the basis for the 4D assignment approach. These spectra were uniformly acquired as described in the Supporting Information. They are used to filter the 4D (H)COCANH, (H)CACONH, and (H)CBCANH spectra for genuine peaks to determine the chemical-shift assignment of residues i and $i-1$. Poisson-gap sampled schedules for the indirect dimensions of the non-uniformly sampled experiments were generated by using the hmsIST software.[33] The number of points was calculated according to the required spectral widths and chosen acquisition times (6.9 ms for ^{13}CO, 5.2 ms for ^{13}Cα, 10.7 ms for ^{15}N and 4.4 ms for ^{13}Cβ were selected). All schedules were created with a sinusoidal weight of 2. (H)COCANH and (H)CACONH were sampled with a density of 10% and (H)CBCANH with only 2%. The collected FIDs were processed in the direct dimension with nmrPipe,[34] and missing spectral points were reconstructed with the hmsIST software package[35] (See the Supporting Information for details: Figures S2–S4, Tables S1–S5, and Pulse program S1).

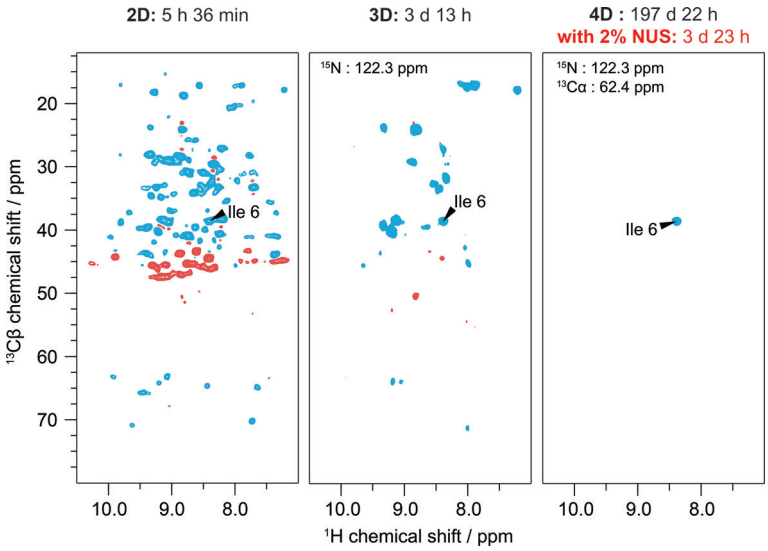

Figure 3. Comparison of (H)CBCANH experiments with different dimensionalities (2D, 3D, and 4D). Increasing dimensionality reduces the spectral crowding in the 2D spectral planes (for the 3D and 4D: projected from the 4D data set) but at the same time exponentially prolongs the experimental time if uniform sampling is used. The non-uniform sampling approach overcomes the 4D barrier through the acquisition of only 2% of the data points that are required in the traditional approach. Negative peaks in the 2D spectrum result from glycine residues that lack a Cβ atom.

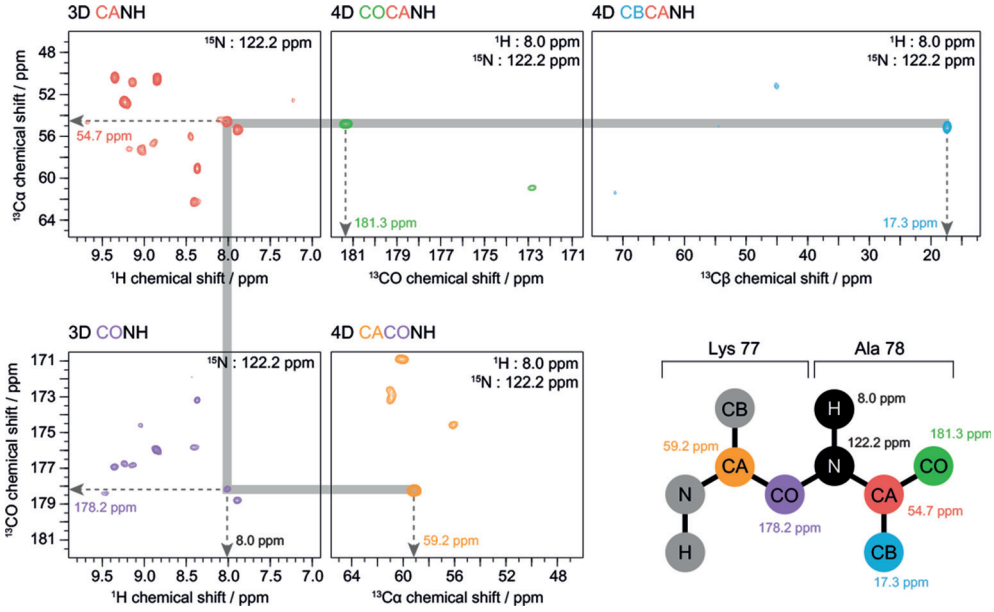

Figure 4. Assignment procedure based on two 3D and three non-uniformly sampled 4D correlation spectra. 3D (H)CANH and (H)CONH spectra serve as starting points in the procedure. In the 3D (H)CANH spectrum, the NH pair of Ala78 is correlated with its intraresidual ^{13}Cα resonance (red). Navigating to the determined ^{1}H, ^{15}N and ^{13}Cα resonances in the 4D (H)COCANH spectrum yields the intraresidual ^{13}CO resonance (green). Navigating to the same resonances in the 4D (H)CBCANH spectrum yields the ^{13}Cβ chemical shift (blue). Note that the ^{13}Cα and ^{13}Cβ chemical shifts in combination are characteristic of an alanine residue. In the 3D (H)CONH spectrum, the same NH pair is correlated with the ^{13}CO chemical shift of the preceding Lys77 residue (purple). The detected ^{1}H, ^{15}N and ^{13}CO chemical shifts are used in the 4D (H)CACONH spectrum to identify the ^{13}Cα chemical shift of the preceding Lys77 residue (orange). The knowledge of intraresidual chemical shifts (i.e., ^{1}H, ^{15}N, ^{13}Cα, ^{13}CO, ^{13}Cβ of residue i) and those of the preceding residue (i.e., ^{13}Cα, ^{13}CO of residue $i-1$) allows the connection of sequential amino acids along the whole chain, in a procedure known as the "backbone walk".

In the 3D (H)CANH spectrum, the $C\alpha_i$ resonance belonging to a specific N_iH_i pair is determined. These three resonances are used in the 4D (H)COCANH and (H)CBCANH spectra to determine CO_i and $C\beta_i$ resonances, respectively. In the 3D (H)CONH spectrum, the CO_{i-1} resonance for the same N_iH_i pair is found. Navigating to these resonances in the 4D (H)CACONH spectrum yields the $C\alpha_{i-1}$ resonance. By this procedure $C\alpha_i$, CO_i, $C\beta_i$, and CO_{i-1}, $C\alpha_{i-1}$ for a given N_iH_i pair can be determined. Using this procedure, the resonances of two consecutive residues (i and $i-1$) are unambiguously connected, assuming that they do not overlap. Subsequently, all residues in the protein are linked in an iterative manner, a procedure known as the "backbone walk". For validation purposes, we have cross-checked the identified sequential NH pairs by means of a 3D (H)N-(CACO)NH spectrum.[36]

The application of this method to gp17.1 allowed extensive backbone resonance assignment (91%) as listed in the Supporting Information. Including multiple conformations, 190 residues could be assigned (Figure S5 and Table S6). The secondary structure was predicted from the assigned chemical shifts using TalosN[37] and is presented in Figure 5. The secondary-structure elements are mapped onto a homology model from previous work, where solution NMR studies of monomeric gp17.1 were conducted and a homology model of the assembled tail tube was proposed.[15] In monomeric gp17.1, only parts of the β-strands, namely β3.2, β5.2, and β6.1, were identified by solution NMR. Signals corresponding to β1, β4, and β5.1 were not observed, probably owing to conformational exchange. Assignment of the remaining residues showed that they have random coil conformation in solution.

Upon polymerization, the gp17.1 protein becomes more structured, and the prospective β-strands and α-helices transform from a random-coil structure into a stable globular fold (Figure S6). In our analysis, we can identify those different secondary structure elements, which are consistent with the proposed homology model (See Figure 5B). Furthermore, we were able to find the formerly unknown β-strands β6.2, β7, β8, and β9 in the C-terminal domain. The secondary chemical-shift analysis also indicates that the loop β2β3 stretches from residue 41 to 51 and is bordered by the two formerly unobserved β-strands β2.2 and β3.1 in the polymerized form. It was reported that deletion of fragment 40–56, which contains β3.1, impairs gp17.1 self-assembly. Moreover, it was shown that in the case of the T4 phage tail tube (another phage tail system), an N-terminal extension to the β-barrel forms an extended segment embracing the next monomer.[38] In the case of gp17.1, this extension seems to be located at the C terminus of the protein, where additional β-strands were found. Thus, we propose that β3.1, β7, β8, and β9 mediate intermolecular interactions.

Second conformations (peak doubling) of more than two consecutive residues are found in β1, β2, β4, β5.2, and β6.1. Since the chemical-shift differences between major and minor conformation (according to peak intensity) seem random and do not indicate a different secondary structure, these might result from slight structural disorder (Table S6). A future 3D structure of the entire gp17.1 tail-tube assembly will give insight into their origin.

We expect that the application of the introduced approach to even larger or more heterogeneous systems would be possible, since the analysis after data acquisition turned out to be very straightforward for gp17.1. We note that our approach may also offer advantages for the study of complex materials such as bone[39] or RNA and RNA–protein complexes, which can be challenging for NMR analysis due to the presence of only four different building blocks.[40,41] We also envisage the application of similar experiments to the analysis of chemical-shift anisotropy (CSA) tensors, where one additional dimension is needed for the CSA recoupling, and the CSA dimension requires large spectral widths.[42]

Acknowledgements

We thank Dr. Veniamin Chevelkov and Eve Ousby for valuable discussions. This work was supported by the Leibniz-Forschungsinstitut für Molekulare Pharmakologie (FMP) and the European Research Council (ERC Starting Grant to A.L.).

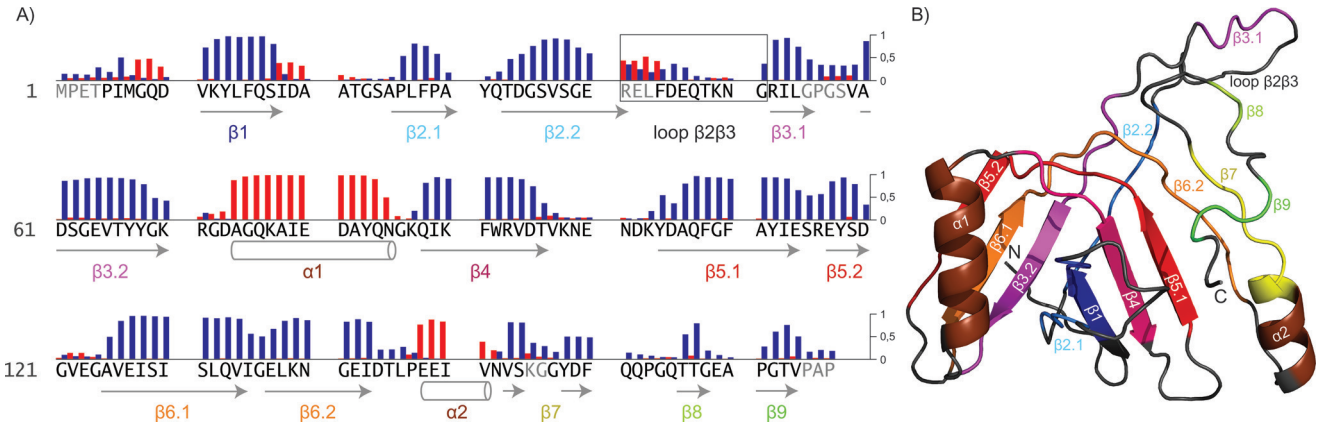

Figure 5. Secondary-structure analysis of polymerized gp17.1 tail-tube protein. A) TalosN secondary structure prediction. Gray letters represent unassigned residues. Blue bars represent the probability of β-sheet structure (arrows), red bars the probability of α-helical structure (barrels). The His-tag is not shown. B) Homology model of a polymerized gp17.1 subunit taken from Langlois et al.[15] Secondary-structure elements from (A) are mapped onto the model in corresponding colors. Elements and N and C termini are labeled.

Conflict of interest

The authors declare no conflict of interest.

Keywords: bacteriophage · gp17.1 · non-uniform sampling · protein structures · solid-state NMR

How to cite: *Angew. Chem. Int. Ed.* **2017**, *56*, 9497–9501
Angew. Chem. **2017**, *129*, 9625–9629

[1] A. K. Schütz, T. Vagt, M. Huber, O. Y. Ovchinnikova, R. Cadalbert, J. Wall, P. Güntert, A. Böckmann, R. Glockshuber, B. H. Meier, *Angew. Chem. Int. Ed.* **2015**, *54*, 331–335; *Angew. Chem.* **2015**, *127*, 337–342.
[2] M. T. Colvin, R. Silvers, Q. Z. Ni, T. V. Can, I. Sergeyev, M. Rosay, K. J. Donovan, B. Michael, J. Wall, S. Linse, et al., *J. Am. Chem. Soc.* **2016**, *138*, 9663–9674.
[3] S. Vasa, L. Lin, C. Shi, B. Habenstein, D. Riedel, J. Kühn, M. Thanbichler, A. Lange, *Proc. Natl. Acad. Sci. USA* **2015**, *112*, E127–36.
[4] C. Shi, P. Fricke, L. Lin, V. Chevelkov, M. Wegstroth, K. Giller, S. Becker, M. Thanbichler, A. Lange, *Sci. Adv.* **2015**, *1*, e1501087.
[5] S. Wang, V. Ladizhansky, *Prog. Nucl. Magn. Reson. Spectrosc.* **2014**, *82*, 1–26.
[6] G. Abramov, O. Morag, A. Goldbourt, *J. Magn. Reson.* **2015**, *253*, 80–90.
[7] J. R. Lewandowski, M. E. Halse, M. Blackledge, L. Emsley, *Science* **2015**, *348*, 578–581.
[8] A. Goldbourt, B. J. Gross, L. A. Day, A. E. McDermott, *J. Am. Chem. Soc.* **2007**, *129*, 2338–2344.
[9] D. Mance, T. Sinnige, M. Kaplan, S. Narasimhan, M. Daniëls, K. Houben, M. Baldus, M. Weingarth, *Angew. Chem. Int. Ed.* **2015**, *54*, 15799–15803; *Angew. Chem.* **2015**, *127*, 16025–16029.
[10] J. Medeiros-Silva, D. Mance, M. Daniëls, S. Jekhmane, K. Houben, M. Baldus, M. Weingarth, *Angew. Chem. Int. Ed.* **2016**, *55*, 13606–13610; *Angew. Chem.* **2016**, *128*, 13804–13808.
[11] B. Bersch, J. M. Dörr, A. Hessel, J. A. Killian, P. Schanda, *Angew. Chem. Int. Ed.* **2017**, *56*, 2508–2512; *Angew. Chem.* **2017**, *129*, 2549–2553.
[12] Z. Golkar, O. Bagasra, D. G. Pace, *J. Infect. Dev. Countries* **2014**, *8*, 129–136.
[13] S. Abedon, S. J. Kuhl, B. G. Blasdel, E. M. Kutter, *Bacteriophage* **2011**, *1*, 66–85.
[14] C. Plisson, H. E. White, I. Auzat, A. Zafarani, C. São-José, S. Lhuillier, P. Tavares, E. V. Orlova, *EMBO J.* **2007**, *26*, 3720–3728.
[15] C. Langlois, S. Ramboarina, A. Cukkemane, I. Auzat, B. Chagot, B. Gilquin, A. Ignatiou, I. Petitpas, E. Kasotakis, M. Paternostre, et al., *J. Biol. Chem.* **2014**, *290*, 3836–3849.
[16] D. H. Zhou, A. J. Nieuwkoop, D. A. Berthold, G. Comellas, L. J. Sperling, M. Tang, G. J. Shah, E. J. Brea, L. R. Lemkau, C. M. Rienstra, *J. Biomol. NMR* **2012**, *54*, 291–305.
[17] V. Chevelkov, B. Habenstein, A. Loquet, K. Giller, S. Becker, A. Lange, *J. Magn. Reson.* **2014**, *242*, 180–188.
[18] E. Barbet-Massin, A. J. Pell, J. S. Retel, L. B. Andreas, K. Jaudzems, W. T. Franks, A. J. Nieuwkoop, M. Hiller, V. Higman, P. Guerry, et al., *J. Am. Chem. Soc.* **2014**, *136*, 12489–12497.
[19] S. Penzel, A. A. Smith, V. Agarwal, A. Hunkeler, M. L. Org, A. Samoson, A. Böckmann, M. Ernst, B. H. Meier, *J. Biomol. NMR* **2015**, *63*, 165–186.
[20] P. Fricke, V. Chevelkov, M. Zinke, K. Giller, S. Becker, A. Lange, *Nat. Protoc.* **2017**, *12*, 764–782.
[21] S. Xiang, V. Chevelkov, S. Becker, A. Lange, *J. Biomol. NMR* **2014**, *60*, 85–90.
[22] S. Xiang, J. Biernat, E. Mandelkow, S. Becker, R. Linser, *Chem. Commun.* **2016**, *52*, 0–3.
[23] S. Xiang, N. Kulminskaya, B. Habenstein, J. Biernat, K. Tepper, M. Paulat, C. Griesinger, S. Becker, A. Lange, E. Mandelkow, et al., *J. Am. Chem. Soc.* **2017**, *139*, 2639–2646.
[24] J. C. J. Barna, E. D. Laue, M. R. Mayger, J. Skilling, S. J. P. Worrall, *J. Magn. Reson.* **1986**, *73*, 69–77.
[25] C. L. Suiter, S. Paramasivam, G. Hou, S. Sun, D. Rice, J. C. Hoch, D. Rovnyak, T. Polenova, *J. Biomol. NMR* **2014**, *59*, 57–73.
[26] S. Sun, S. Yan, C. Guo, M. Li, J. C. Hoch, J. C. Williams, T. Polenova, *J. Phys. Chem. B* **2012**, *116*, 13585–13596.
[27] B. Worley, *J. Magn. Reson.* **2016**, *265*, 90–98.
[28] V. Y. Orekhov, I. V. Ibraghimov, M. Billeter, *J. Biomol. NMR.*, **2001**, 49–60.
[29] K. Kazimierczuk, V. Y. Orekhov, *Angew. Chem. Int. Ed.* **2011**, *50*, 5556–5559; *Angew. Chem.* **2011**, *123*, 5670–5673.
[30] S. G. Hyberts, H. Arthanari, S. A. Robson, G. Wagner, *J. Magn. Reson.* **2014**, *241*, 60–73.
[31] M. Huber, S. Hiller, P. Schanda, M. Ernst, A. Böckmann, R. Verel, B. H. Meier, *ChemPhysChem* **2011**, *12*, 915–918.
[32] R. Linser, B. Bardiaux, V. Higman, U. Fink, B. Reif, *J. Am. Chem. Soc.* **2011**, *133*, 5905–5912.
[33] S. G. Hyberts, K. Takeuchi, G. Wagner, *J. Am. Chem. Soc.* **2010**, *132*, 2145–2147.
[34] F. Delaglio, S. Grzesiek, G. W. Vuister, G. Zhu, J. Pfeifer, A. Bax, *J. Biomol. NMR* **1995**, *6*, 277–293.
[35] S. G. Hyberts, A. G. Milbradt, A. B. Wagner, H. Arthanari, G. Wagner, *J. Biomol. NMR* **2012**, *52*, 315–327.
[36] Z. Y. J. Sun, D. P. Frueh, P. Selenko, J. C. Hoch, G. Wagner, *J. Biomol. NMR* **2005**, *33*, 43–50.
[37] Y. Shen, A. Bax, *J. Biomol. NMR* **2013**, *56*, 227–241.
[38] N. M. I. Taylor, N. S. Prokhorov, R. C. Guerrero-Ferreira, M. M. Shneider, C. Browning, K. N. Goldie, H. Stahlberg, P. G. Leiman, *Nature* **2016**, *533*, 346–352.
[39] R. Zhang, K. H. Mroue, A. Ramamoorthy, *Acc. Chem. Res.* **2017**, acs.accounts.7b00082.
[40] A. Marchanka, B. Simon, T. Carlomagno, *Angew. Chem. Int. Ed.* **2013**, *52*, 9996–10001; *Angew. Chem.* **2013**, *125*, 10180–10185.
[41] A. Marchanka, B. Simon, G. Althoff-Ospelt, T. Carlomagno, *Nat. Commun.* **2015**, *6*, 7024.
[42] M. K. Pandey, Y. Nishiyama, *J. Magn. Reson.* **2015**, *261*, 133–140.

Manuscript received: June 14, 2017
Accepted manuscript online: June 23, 2017
Version of record online: July 7, 2017

